



The impact of previously prepared potassium and iron in nano forms using gamma radiation on growth and productivity of green bean

A.M. M. El-Tanahy^{1*}, N. M. Marzouk¹, M. Salah² and A. M. Mounir³.

1. Vegetable Research Department -Agricultural and Biological Research Institute- National Research Center. Giza.

Egypt

2. Polymer Chemistry Department-National Center for Radiation Research and Technology-Egyptian Atomic Energy

Authority-Cairo-Egypt

3. Natural Products Research Department- National Center for Radiation Research and Technology- Egyptian Atomic

Energy Authority-Cairo-Egypt

Abstract

Potassium and iron oxide nanoparticles were prepared via gamma irradiation using PVA and PVP as stabilizers and capping agent to control the size of the particles. HRTEM indicated the formation of potassium and iron oxide nanoparticles within the polymeric network of PVA and PVP with mean sizes 12 nm and 2.38 nm, respectively.

The ultraviolet visible (UV-vis) spectroscopy measurements show a distinct characteristic absorption peak indicating the formation of potassium and iron oxide nanoparticles. As for the agricultural application, an experiment was carried out during the two successive seasons of 2019 and 2020 seasons at National Research Centre's experimental Station, El Nobaria Region, Behira Governorate, Egypt. Results show that 8 ml/l of nano potassium and 9 ml/l of nano iron oxide scored the highest values of plant length, number of leaves and branches, total plant fresh weight, dry matter percentage and chlorophyll reading. As for pod yield and its component the same both previous concentrations gave the highest pod length, pod number per plant, pod fresh and dry weight and total yield per feddan. Also, both concentrations gave higher protein percentage, total soluble solids percentage, potassium percentage and iron concentration as well as lower fiber percentage than other treatments.

Keywords: Nano potassium, nano iron oxide, gamma radiation, green bean

1. Introduction

The massive production of vegetable crops in newly reclaimed soils depends on many factors, one of these factors is the addition and the consumption of high levels of fertilizers that contain either macro or microelements. The excessive addition of chemical fertilizers has a downside effect

on the environmental system and beneficial microorganisms in soil which affects the fertility of the soil and its production [1]. On the other hand, it was found the extravagant addition of macro element like nitrogen, phosphorus, and potassium is not efficacious at the rate of 20 -50 % for nitrogen, 10 - 25% for phosphorus, and 70 - 80 % for potassium [2, 3]. The low useful consumption of the previous fertilizers might be referred to leaching, hydrolysis or denitrification.

*Corresponding author e-mail: atanahy@hotmail.com.; (A. M. M. El-tanahy).

The new scientific revolution in fertilizers sector which was accompanied by the appearance of nanotechnology as a new technique, led to an increase and enhancement of fertilizers which increase the production with low damage to the environment [4], through changing the physico-chemical properties of nano elements compared to their essential elements [5] and differ than the same elements in their volumetric diameter [6].

The fertilizer could be considered in nano form when its particles are under 10 nm in size, it could be used as nano fertilizer which is characterized by its effectiveness in absorbance, slow release and stress tolerance [7].

Nano fertilizers could be considered as non-traditional products which prevent the environment from the pollution of traditional fertilizers. These nano fertilizers are prepared from traditional fertilizers through chemical, physical or biological processes which lead to obtain superior results than traditional fertilizers concerning addition rates and nutrient uptake [8]. The benefit of nano fertilizers usage could be summarized in protecting the soil from the excessive addition of traditional fertilizers, enhancing use efficiency of elements and diminishing the amount of additive fertilizers as a result of their high surface area and their nano particle size [9]. On the other hand, nano fertilizers have an effective role in plant nutrition through their ability to be a slow release fertilizers that provide plants with their abundant amount of minerals [10]. The structure of new reclaimed soils (sandy soil) obligate the farmers to use slow or controlled release fertilizers which have higher reactivity, more specific surface area, more density of reactive area which enhance the reactivity of these area on particle surface [5], or through the foliar application treatments of macro and micro elements.

The interaction between different crops and fertilizers in nano form which affect the morphological and physiological changes depends on the characters of nano particles. The influence of nano particles on crops depends on their chemical constituents, size, surface covering, reaction between elements and plants and finally the determined dose which affects the physiological process and led to an effective influence on plant [11]. Thus, the application of nano fertilizers in agriculture sector, gave the chance to improve the absorption of different fertilizers and get the most out of them, reducing costs and protect the ecosystem.

Potassium in one of the most important macro elements which has a main role in photosynthesis, nitrogen metabolism, sugar translocation,

the activation of several enzymes, stomatal opening and closure as well as growth of meristematic tissues. Potassium particles ranging from 50 to 150 nm in water sector, pore diameters of plants cell wall ranging from 5 to 20 nm in water sector [12].

Iron is one of the main micronutrients in plant, it has an important role in biological functions of many enzymes that participate in several vital processes such as photosynthesis, protein building called heme- and non-heme protein, this heme protein consists of cytochrome oxidase, catalases, peroxidases and leghemoglobins that play an important role in regulating and scavenging reactive oxygen species (ROS) and fixing nitrogen in root nodules of legumes through symbiosis reaction between plants and rhizobium bacteria [13] and respiration process as well as enhancing the quality of plant yield [14]. The deficit of iron causes a defect in chlorophyll synthesis, its surplus causes a generation of ROS which leads to an oxidative stress in plant [15]. On the other hand, iron nano particles are able to enhance the absorption of minerals and enhance the photosynthesis [16].

Most of agricultural soil has an abundant proportion of iron, but 30% of this proportion is in unavailable form for crop absorption and fixed to soil particles [17]. Iron is presented in the form of Fe^{3+} in alkaline soil with high pH value which making it in unavailable form for plant, that absorbs Fe^{2+} element [18].

Present-day NP platforms are often categorized into three major groups including: (i) inorganic-based (solid) nanoparticles (non-biodegradable); (ii) organic-based nanoparticles (extremely biodegradable); and (iii) hybrid nanoparticles. Organic-based nanoparticles, which are most often utilized in agriculture, include generally of water-soluble biodegradable biocompatible polymers, like chitosan, lignin, phospholipids, lecithin, lactalbumin, starch, cellulose derivatives, alginates, polylactides, poly(propylene glycol), polyacrylamide and polysorbate. The nano-formulations supported biodegradable organic-based matrices prepared by encapsulation technology allow designing controlled-release nano carriers, during which the surface is often modified by various other molecules. Utilization this technique not only aqueous solubility (lipophilicity or hydrophilicity) of the active ingredient is often modified, but also its targeted bio distribution are often ensured; thus, the dosage of agrochemical are often reduced, because matrices add protection of the active from environment and the other way around.

Gamma radiation is one of the types of ionizing radiation. It was employed previously to polymerize water-soluble unsaturated polymers and

produce the cross-linked structure. It has been shown that reaction of intramolecular cross-linking is often administered with water-soluble polymers in dilute solutions (polymer concentration must be below enough to avoid intermolecular cross-linking) [19]. The technique mainly relies on producing free radicals within the polymer following exposure to a high energy sources like gamma rays. The effect of radiation (direct or indirect) will depend upon the polymer environment. Recently, it has been recommended to believe the radiation-induced intramolecular crosslinking of single polymer chains as an alternate approach to the formation of sub-micron-size polymer gels [20].

PVP is one among the many capping agents that are utilized in nanotechnology to beat drawbacks related to conventional methods of preparation of nanoparticles like their toxicity, size, and agglomeration. Hence, eco-friendly nano-formulations are obtained using PVP having more applicability [21]. In various researches, PVP has been employed as a capping agent around metal nanoparticles like Iron (Fe), silver (Ag), gold (Au), zinc (Zn), etc. [22].

PVA is one among the high-performance capping agents utilized in nanotechnology [23]. PVA may be a synthetic polymer owning great hydrophilicity, biocompatibility, and biodegradability. PVA has been used as a stabilizing agent, for the form and size control of Ag nanoparticles to guard against water [24]. To improve the optical emission, crystallinity, and size dispersion, ZnO nanoparticles capped with PVA were prepared by the sol-gel method.

Green bean is one of the most important vegetable crops of family fabaceae, it is a good source of protein, vitamins and calcium. The total area of cultivated green bean around the world is 1.527 .613 hectares with 21.720.588 tons of production [25]. In Egypt, green bean is considered one of the important export crops and also for local markets , near 3.5 % of the total production of the world produces from Egypt [26].The production of green bean under new reclaimed soils facing some difficulties, one of theme is its sensitivity to potassium and iron deficit.

Thus, the aim of this search was to evaluate the effect of nano gels which were prepared throughout radiation of poly (N-vinyl-2-pyrrolidone) (PVP) and polyvinyl alcohol (PVA) aqueous solutions and investigate the effect of foliar application with both nano potassium and iron oxide on growth and productivity of green bean plants under new reclaimed soil.

Materials and methods

Materials.

Polyvinyl alcohol (PVA) with molecular weight 1, 15,000, (-C₂H₄O)_n by LobaChemie, India. Acetic

acid glacial; M.W. 60.05, with assay (acidimetric) min 99.5% purchased from LobaChemie. Ethanol, ferrous sulfate and potassium sulfate obtained from El Gomhouria Co., Egypt.

Preparation of PVA/ potassium nanoparticles core-shell structure. - This work aimed to evaluate a polymeric solubilizer for agricultural applications. In this study, potassium nanoparticles were embedded with polyvinyl alcohol (PVA). The powdered PVA was dissolved in bidistilled water at 80°C, with continuous stirring. Combination of acetic acid and ethanol were added to the solution. Finally, 10 % w t of potassium sulfate salt was added to the solution with the continued stirring. The resulted solution was exposed to gamma radiation dose 4 kGy(Indian cell - ⁶⁰Co) separately with dose rate of 1.16KGy/h., at NCRRT, Cairo, Egypt to obtain the core shell nanostructure [27,28]

Preparation of PVP/ iron oxide nanoparticles.

14% (v/v) of acetic acid was added to an equivalent amount of bidistilled water. Also, 2.5% of Polyvinylpyrrolidone (PVP) was added via continuous stirring at 70°C. After dissolving of PVP, an equivalent amount of Glycerin (glycerol) was added. Finally, after fully mixing of the components, 10% (w/w) of ferrous sulfate was added to the solution with the continued stirring. The resulted solution was exposed to gamma radiation dose at 4 kGy (Indian cell - ⁶⁰Co) separately with dose rate of 1 Gy / 4.14 sec., at NCRRT, Cairo, Egypt[27, 28].

Characterization.-High Resolution Transmission electron microscopy (HRTEM)

High Resolution Transmission electron microscopy (HRTEM) measurements were performed with (JEOL, JEM 2100, Japan) operating at 200 kV. HRTEM was used to find out the distribution and size of iron nanoparticles.

UV-Vis absorption spectra.

The UV-Vis absorption spectra were taken by double beam spectrophotometer provided with computer data acquisition Type JASCO 670UV-Vis/NIR.

FT-IR spectroscopy.

FTIR was carried out by using FT-IR 6300, Jasco, Japan in the range 400-4000 cm⁻¹.

Agricultural study.

The experiment was carried out during 2019 and 2020 seasons at National Research Centre's Experimental Station, El Nobaria Region, Behira Governorate, Egypt. Physical and chemical analyses of soil is presented in Table 1.

Plant materials.

This experiment was conducted in newly reclaimed sandy soil, seeds of green bean cv. Bronco were sown in two sides of soil beds, 40 cm width at 10 cm apart within the plant rows on the 1st of March during the two successive seasons. Drip lines placed above soil surface at 1.5 meter apart in each row in the middle

of soil beds. The agricultural practices were carried out according to the recommendation of Egyptian Ministry of Agriculture and Land Reclamation. Calcium super-phosphate (15% P₂O₅) at 300Kg per feddan was added one time during soil preparation. Ammonium nitrate (33%N) at 250Kg per feddan and potassium sulphate (48%K₂O) at 100Kg K₂O per feddan were applied during the growth season.

Treatments and experimental design.

Four foliar applications of nano potassium (control, 2, 4 and 8ml/l) and nano iron oxide(control, 3, 6 and 9 ml/l) were sprayed at 21 days after sowing then 10 and 20 days after the first foliar application. The experiment consisted of 16 treatments with three replicates. The experiment was laid out in a split plot design where nano potassium treatments were arranged in main plots while nano iron oxide treatments randomly were distributed in sub-plots. The area of the experimental plot was 12.8 m².

Vegetative characteristics.

Samples of 6 plants were taken randomly at 45 days after sowing (flowering stage) from each experimental plot for measuring: Plant length, number of leaves and branches per plant, total fresh weight and dry matter percentage of plant was estimated according to the following formula: Plant dry matter% = (plant dry weight / plant fresh weight) x 100, as well as total chlorophyll reading of the sixth mature leaf through chlorophyll meter (SPAD-501).

Green Pod Yield and its components.

At harvest stage (60 days after sowing), green pods were collected for estimated: pods fresh and dry weights (g) and total green pods yield/feddan (ton). A sample of 100 green pods at second picking were randomly taken, average pod length (cm) and diameter (cm) were recorded.

Nutritional Value.

A sample of 50 green pods at second picking were randomly taken to record: Total soluble solids (TSS %) which was obtained using hand refractometer according to the method described by A.O.A.C. [29] pods fiber percentage was determined according to Rai and Mudgal [30]. Total protein percentage in pods was determined as a factor of 6.25 which was used for converting the total nitrogen percentage to protein percentage [29], potassium percentage was determined according to Brown and Lillie [31] and iron concentration was determined according to Chapman and Pratt [32].

Statistical analysis.

All data were subjected to statistical analysis using MSTATC Computer Program [33]. The Duncan's New Multiple Range test at 5% level of probability was used to test the significance of differences among mean values of treatments [34].

Results and discussion.

High Resolution Transmission electron microscopy (HRTEM)

Transmission electron microscopy (TEM) is considered to be the most popular technique in characterizing nanomaterials in electron microscopy. The HRTEM analysis was used to visualize the size and shape of the synthesized potassium nanoparticles. It is also possible to produce an image from electrons deflected by a particular crystal plane. Figure 1 (a, b) show the morphology of the synthesized PVA/potassium nanoparticles core-shell structure nanogel which was examined by HRTEM. The potassium nanoparticles seem to be well surrounded by the PVA shell matrix. It is clear from the Figure that, potassium nanoparticles formed in the PVA shell networks have a cubic shape, and lower than 30 nanometers in size [35, 36].

Figure 1 (c, d) show the SAED pattern. The electron diffraction pattern shows characteristic concentric rings as bright spots, which is associated with the crystalline nature of potassium. In addition, from Figure 1, it is clear that the core potassium particles are about 6.8 nm in diameter [37].

The size distribution plots were fit employing a Gaussian model with Microcal Origin 5.0 graphing software to work out the widths and centers of the dimensions distributions. The width of the distribution gives a thought of how narrow or wide the dimensions distribution is and therefore the center of the distribution is that the most probable or average size of the nanoparticles (depending on the form of the distribution). Pertaining to the dimensions of the nanoparticles, Figure 2 illustrates the dimensions distribution histogram of nanoparticles. It is often noticed that the potassium nanoparticles size was within the range between 7-27 nm.

The bulk size of potassium nanoparticles was found around 12 nm. The tiny size of potassium nanoparticles, which was obtained from the HRTEM image, indicates good stabilization of potassium nanoparticles in PVA nanogel solution [35, 38]. HRTEM images of iron oxide nanoparticles are shown in Figure 3.

Figure 3(a, b, c, and d) showed TEM images of the iron oxide nanoparticles synthesized by gamma radiation. The morphologies of iron oxide nanoparticles showed quasi-spherical, rhombohedral shape and kite rhombus shape, with homogeneous dispersed distribution. Figure 3(d) elucidates the corresponding size of iron oxide nanoparticles. The size values of iron oxide were observed to be around 2.38 nm [39, 40].

The inter-planar spacing of the lattice fringes in Figure 3(g) is 0.26 nm, which are in good agreement with the distances of the (3 1 1) plane of

magnetite (Fe_3O_4) nanoparticles. Figure 3(h) shows the corresponding SAED pattern, suggesting the crystalline structure of the obtained Iron oxide nanoparticles. It is a known fact that polycrystalline materials show a ring pattern whereas single crystal materials show a spotty diffraction pattern in SAED. Accordingly, SAED pattern show polycrystalline structure from iron oxide nanoparticles embedded in PVP network. It has been confirmed by the SAED (selected area electron diffraction) in the Figure 3(h) and this d-spacing value has been calculated via the two opposite bright points of the same circle. Moreover, this d-spacing (inter-planar distance) value (0.26 nm) has been evidenced by using the IFFT method (inset in Figure 3(h and i) and its corresponding values [41].

The size distribution plots were fit using a Gaussian model with Microcal Origin 5.0 graphing software to determine the widths and centers of the size distributions. The width of the distribution gives an idea of how narrow or wide the size distribution is and the center of the distribution is the most probable or average size of the nanoparticles (depending on the shape of the distribution). According to the iron oxide nanoparticles size, Figure (4) represents the size distribution histogram of nanoparticles. It can be showed that the iron oxide nanoparticles size was in the range between 1-6 nm. The majority size of iron oxide nanoparticles was found around 2.4 nm. The small size of potassium nanoparticles, which was obtained from the HRTEM image, indicates a good stabilization of iron oxide nanoparticles in PVP nanogel solution [42,43].

FT-IR measurement.

FTIR is an extremely useful analytical technique used to identify organic, polymeric, and in some cases inorganic materials. The technique is based upon the identification of functional groups within molecules where such groups vibrate (either through stretching or bending in various ways) when irradiated with specific wavelengths of light. The functional groups of the composition PVP/acetic acid /glycerin containing iron oxide nanoparticles was confirmed by **FT-IR spectroscopy.**

Figure (5) shows the characteristic stretching band of PVP existing at 1652.5 cm^{-1} belong to the pyrrolidone C=O group. Other major bands comprise those corresponding to the C–N stretching vibrations absorption of PVP at 1277.5 cm^{-1} , and the absorption peak at 1390.8 cm^{-1} due to the C–H bond in PVP [44,45]. Moreover, The FTIR absorption spectra PVP show weak absorption peaks located at 2946.5 cm^{-1} and a broad band centered at 3434.8 cm^{-1} , which

due to –CH asymmetric stretching vibration and –OH symmetric stretching peaks, respectively [46,47]. The bands at 1038 cm^{-1} , 993 and 918.98 cm^{-1} are related to the C–O stretching vibration of C–O–C groups. Further, the peak at 1108.5 cm^{-1} is due to C–O stretch. The band at 2882 cm^{-1} arises from the bending and scissoring vibrations of CH_2 [48]. The characteristic absorption peak of the carbonyl group of acetic acid is observed at 1716 cm^{-1} . There is a peak at 605.78 cm^{-1} which is due to the new chemical bonds formed between Fe_3O_4 , C–N groups and also C=O groups of PVP [41,49].

FT-IR spectroscopy was used in order to study the function groups of PVA matrix and the interactions between PVA matrix and potassium NPs which achieved via gamma irradiation process. FT-IR spectrum of PVA/ acetic acid/ ethanol contains potassium nanoparticles is shown in Figure 6. The broad band between 3288 and 3600 cm^{-1} represents O–H stretching (intermolecular bonded). The weak peaks at 2617 and 2075 cm^{-1} are attributed to S–H stretching (thiol) resulting from sulfate group of potassium sulfate which was used as a precursor for potassium nanoparticles [50,51]. The peak at 1714 cm^{-1} is due to the stretching C=O from carboxylic acid. The band at about 1639 cm^{-1} is assigned to C=C stretching from alkene. The band corresponding to O–H bending from carboxylic acid and alcohol appear at about 1389 cm^{-1} . The band corresponding to CH_2 symmetric twisting occurs at about 1275 cm^{-1} . The peak presented at 1100 cm^{-1} is assigned to C–O stretch for secondary alcohol. C–O–C stretching band is appeared at 1016 cm^{-1} [44, 21]. Finally, the peak centered at 617 cm^{-1} is related to $\delta(\text{COO}^-)$.

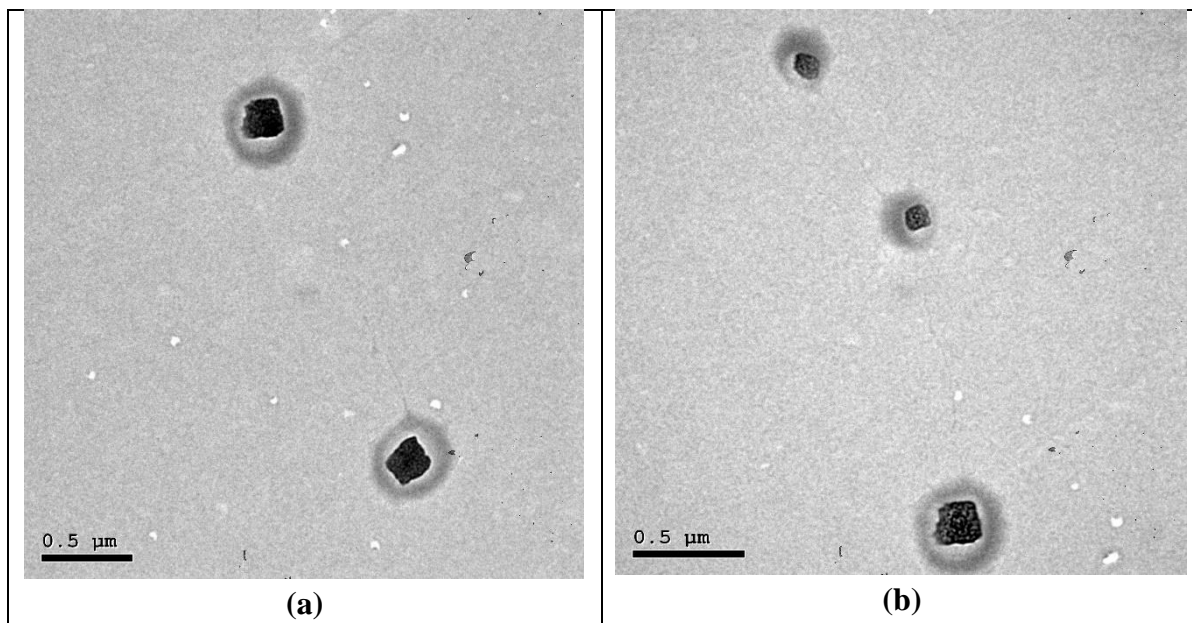
UV-Visible spectroscopy measurements.

UV-Visible spectroscopy (UV-Vis) measures the scattering or absorption of the light passing through a sample. Nanoparticles have unique optical properties which are sensitive to the size, shape, concentration, agglomeration, and refractive index near the nanoparticle surface, which motivates UV-Vis to be a valuable tool for identifying, characterizing, and studying Plasmonic nanoparticles loaded hybrid microgels or nanogels. The measured absorbance spectra spectrophotometer in the wavelength region 200-1400 nm for PVP nanostructure with potassium sulfate is shown in Figure (7).

In Figure 7, the first absorption peak in the spectrum mainly consists of absorption by KOH nanoparticles at 272 nm, but the absorption band of K nanoparticles were also observed around wavelength of 400.

Table 1: Physical and chemical analysis of the experimental soil of El Nobaria Region, Behira Governorate during 2019 and 2020 seasons.

Physical properties							
Particle size distribution							
	Sand%	Clay %	Silt %	Texture			
	73.15	6.1	20.75	Sandy			
Chemical analysis							
Depth (cm)	pH 1:2.5	EC dSm ⁻¹	CaCO ₃ %	CEC C mole Kg ⁻¹	O.M %		
0-15	7.63	0.98	3.22	4.95	0.04		
15-30	7.30	1.09	2.76	4.32	0.02		
Samples (cm)	Macronutrients (%)			Micronutrients (ppm)			
	N	P	K	Fe	Zn	Mn	Cu
0-15	2.10	0.53	1.19	231	145	322	76
15-30	2.11	0.69	1.68	324	172	286	41



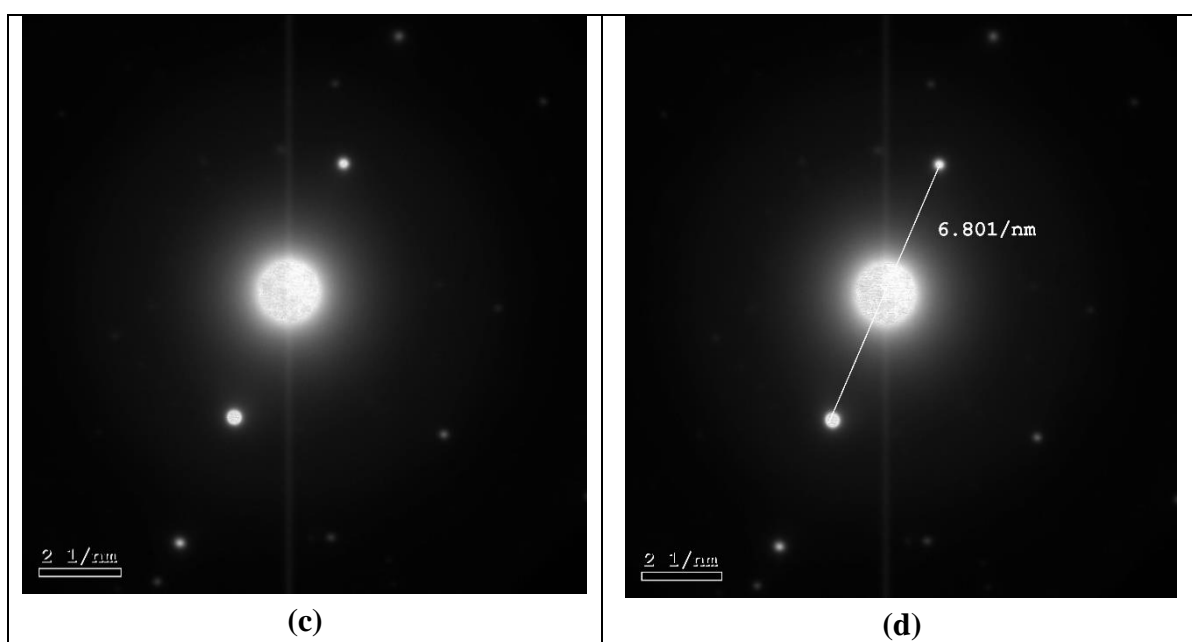


Figure 1: show HRTEM photographs for (a, b) PVA/ potassium nanoparticles core-shell structure and (c, d) SAED pattern for potassium nanoparticles.

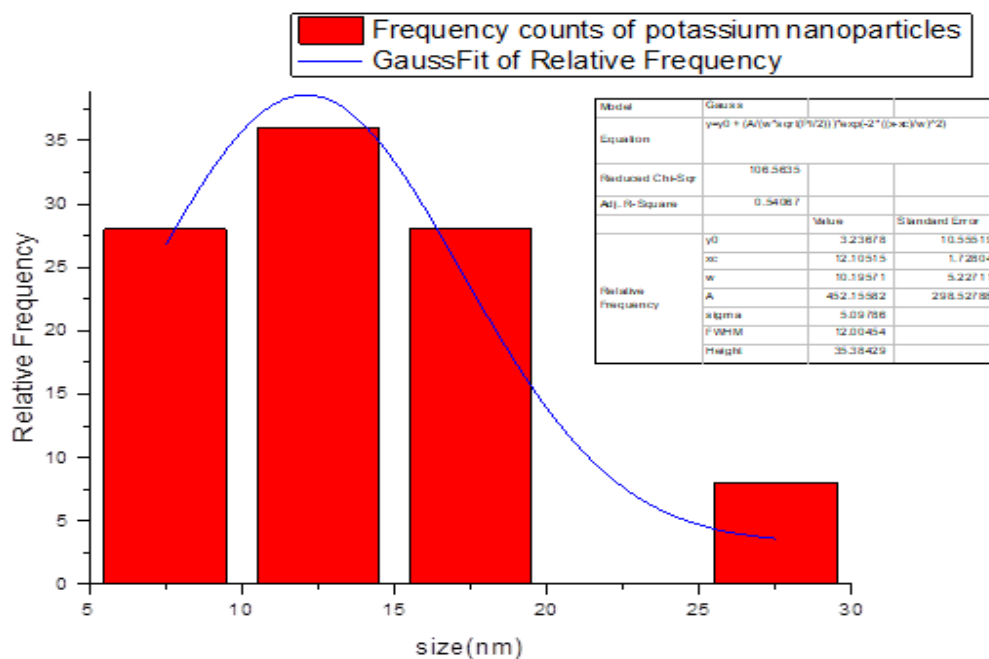
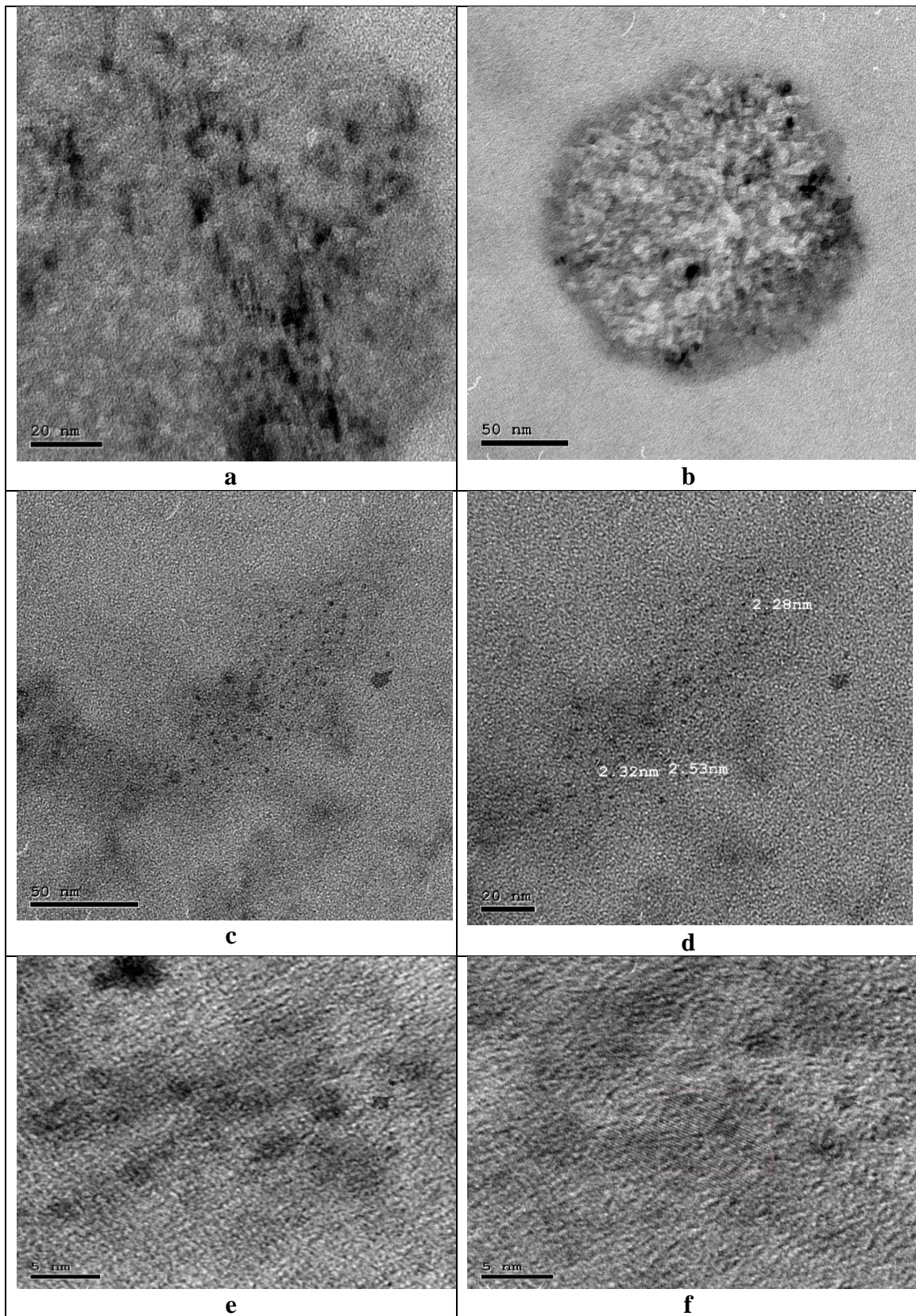


Figure 2: Gaussian fits of size distributions of potassium nanoparticles.



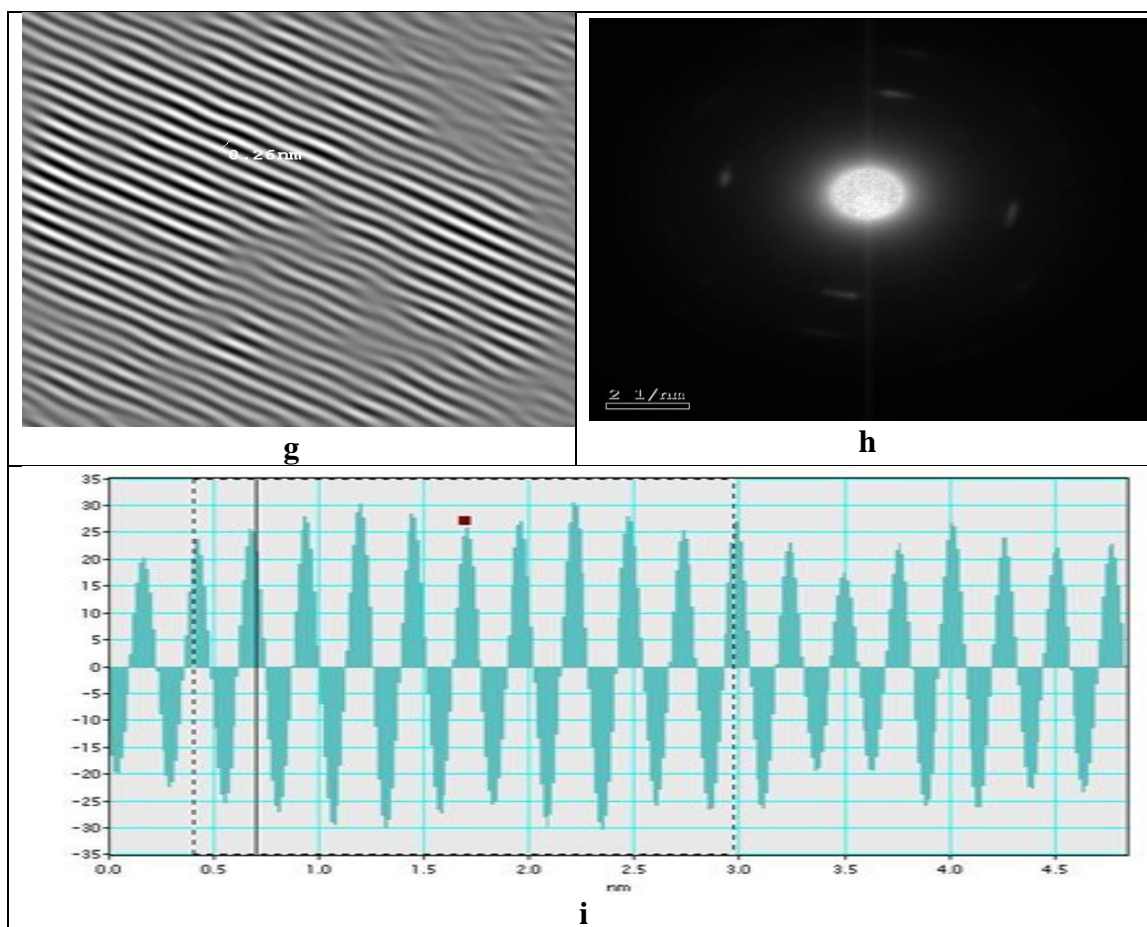


Figure 3: (a, b and c) HRTEM images for PVP/ iron oxide nanoparticles, (d) corresponding size of selected three particles of iron oxide nanoparticles, (e, f, and g) The image corresponds to iron oxide NPs lattice fringes which corroborates the d-spacing value of 0.26 nm, images (h and i) SAED pattern for iron oxide NPs and its IFFT (inset) evidences the d-spacing value.

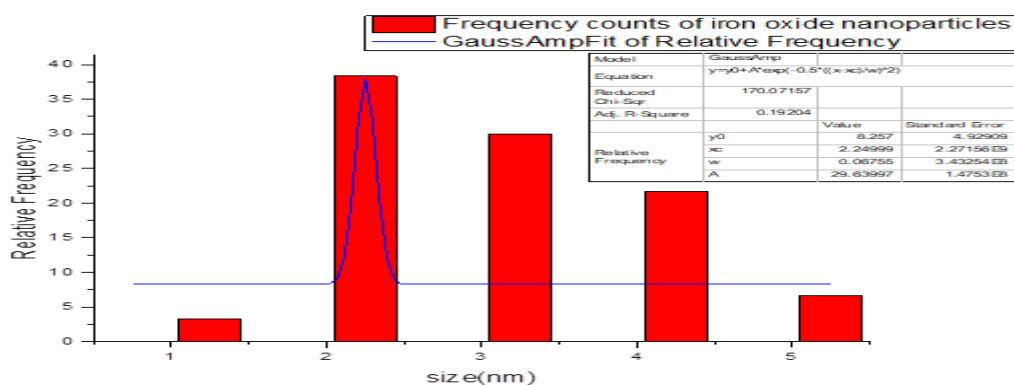


Figure 4: Gaussian fits of size distributions of iron oxide nanoparticles.

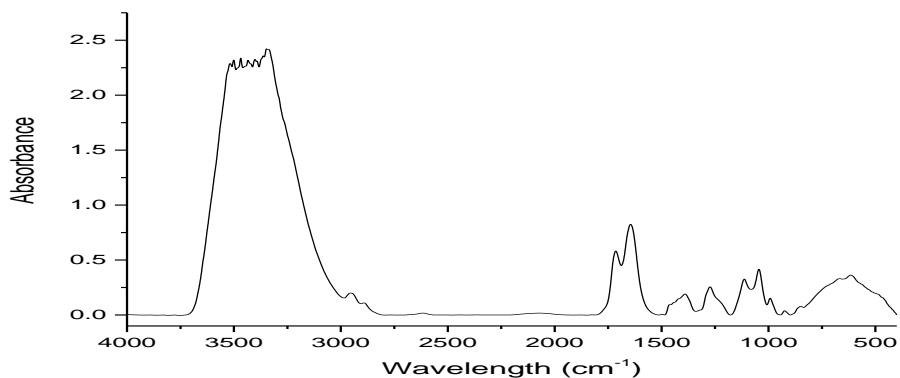


Figure 5: FTIR spectra of PVP/acetic acid /glycerin containing iron oxide nanoparticles.

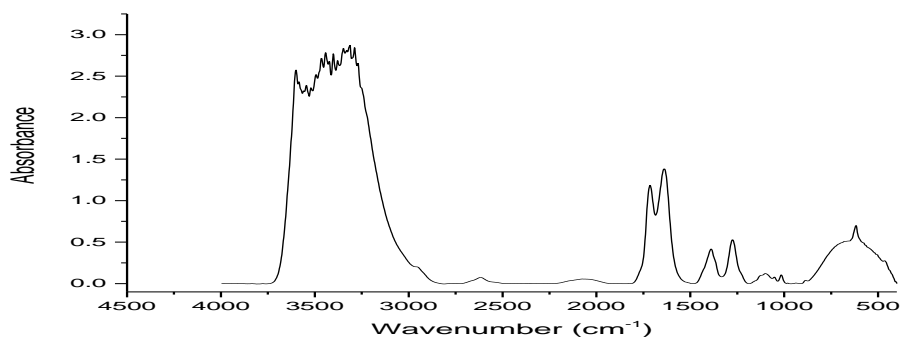


Figure 6: FTIR spectra of PVA/acetic acid /ethanol containing potassium nanoparticles.

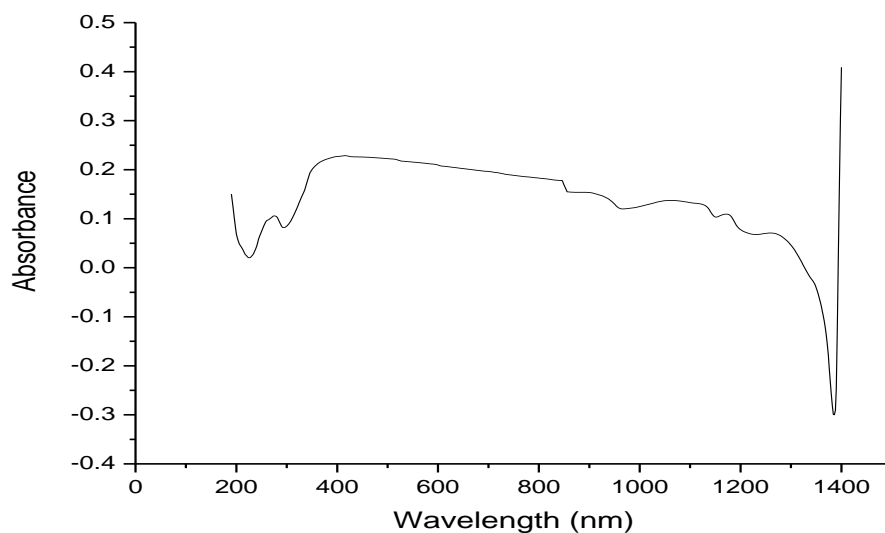


Figure 7: UV spectra of PVA/ potassium nanoparticles.

Table(2):Effect of nano potassium and iron oxide foliar application on plant length(cm),number of leaves , number of branches, total plant fresh weight(g), dry matter (%) and chlorophyll reading (SPAD) of green bean plants during 2019 and 2020 seasons

Characters	Season		First season					Second season				
	Treatments		K					K				
	(ml/l)		Control	2	4	8	Mean	Control	2	4	8	Mean
Plantlength (cm)	Fe	Control	41.20h	41.30h	44.30f	44.10f	42.70D	42.40h	41.30i	43.10h	45.10f	42.90D
		3	43.10g	43.30g	46.40e	46.90e	44.90C	44.30g	44.50g	47.60e	48.10d	46.10C
		6	47.70de	45.50ef	50.10d	51.70d	48.70B	48.90d	49.70c	51.30bc	51.80bc	50.40B
		9	53.00c	54.20b	55.10ab	56.30a	54.60A	52.10b	49.80c	53.20ab	54.20a	52.30A
		Mean	46.20C	46.00C	48.90B	49.70A		46.90C	46.30C	48.80B	49.80A	
Number of leaves	Fe	Control	12.60h	13.90g	14.10f	14.60f	13.8D	11.00i	13.00h	13.20h	13.90g	12.70C
		3	15.30e	16.70e	17.80de	17.90de	16.90C	15.20f	15.80f	16.90e	17.60d	16.30BC
		6	18.10d	19.50c	19.70c	19.80c	19.20B	17.20d	17.40d	17.80d	18.10c	17.60B
		9	19.80c	20.20b	21.50a	21.70a	20.80A	18.90c	20.10b	20.60b	21.80a	20.30A
		Mean	16.40C	17.50B	18.20A	18.50A		15.50C	16.50B	17.10AB	17.80A	
Number of branches	Fe	Control	3.10g	3.60f	4.10e	4.50cd	3.80D	3.30g	3.10g	4.30f	4.60f	3.80D
		3	4.30d	4.60cd	4.80c	4.90c	4.60C	4.50f	4.80d	5.00c	5.10c	4.80C
		6	5.10b	5.00b	5.20b	5.10b	5.10B	5.30b	5.20b	4.90d	5.00c	5.10BC
		9	5.20b	5.40ab	5.50ab	5.70a	5.40A	5.10c	5.60ab	5.70ab	5.90a	5.50A
		Mean	4.40B	4.60B	4.90AB	5.00A		4.50D	4.60C	4.90B	5.10A	
Total plant fresh weight (g)	Fe	Control	52.10h	53.40h	55.60g	56.20f	54.3D	51.70g	52.00g	55.20f	55.80f	53.60D
		3	56.30f	56.90f	59.40e	60.10d	58.1C	56.10e	56.50e	58.40d	59.70d	57.60C
		6	61.80c	61.20c	63.20b	64.20a	62.6B	60.90c	60.80c	62.80b	63.80ab	62.00B
		9	62.30bc	61.70c	63.70b	64.70a	63.1A	61.40c	61.30c	63.30ab	64.30a	62.60A
		Mean	58.10D	58.30C	60.40B	61.30A		57.50C	57.60C	59.90B	60.90A	
Dry matter (%)	Fe	Control	11.80g	12.50f	13.20e	14.10d	12.90C	12.10f	12.80f	13.50e	13.70e	13.00D
		3	14.30d	14.60d	15.20c	15.90c	15.00B	13.90e	14.80d	15.50c	16.20b	15.10C
		6	16.10bc	16.20bc	16.40b	16.80ab	16.30A	16.70b	16.50b	16.80b	17.10ab	16.70B
		9	16.30b	16.40b	16.60b	17.00a	16.60A	17.20ab	17.00ab	17.30ab	17.60a	16.10A
		Mean	14.60B	14.90B	15.30A	15.90A		14.90C	15.20B	15.70B	16.10A	
Chlorophyll reading (SPAD)	Fe	Control	22.20i	24.50h	25.70g	26.70f	24.70D	21.30i	23.60h	24.80g	26.60f	24.00D
		3	27.60e	28.90d	29.60cd	30.30c	29.10C	27.10e	28.00d	28.70d	29.20cd	28.20C
		6	30.90c	31.60bc	32.40b	34.50bc	32.30A	30.30c	30.70c	32.40ab	33.00a	31.70B
		9	31.40bc	32.10b	32.90b	35.00a	32.90A	30.60c	31.00b	32.70ab	33.90a	32.00A
		Mean	28.00D	29.20C	30.10B	31.60A		27.30D	28.30C	29.60B	30.80A	

.Means followed by different letters are significantly deferent at $P \leq 0.05$ level: Duncan's multiple range test.

Table(3):Effect of nano potassium and iron oxide foliar application on pod length(cm), pod number per plant, pod diameter, pod fresh weight(g),pod dry weight (g) and total yield per feddan (ton) of green bean plants during 2019 and 2020 seasons

Characters	Season		First season					Second season				
	Treatments		K					K				
	(ml/l)	Control	2	4	8	Mean	Control	2	4	8	Mean	
Pod length (cm)	Fe	Control	8.90f	9.10f	9.30e	9.50d	9.20D	5.2 h	7.9 g	8.3 f	9.1 e	7.60C
		3	9.50d	9.60d	10.00c	10.50b	9.90C	9.30e	9.40e	9.80d	10.20c	9.60B
		6	10.70b	10.80b	11.30ab	11.60ab	11.10B	10.30c	10.50c	10.90b	11.20ab	10.70AB
		9	11.20ab	11.30ab	11.80ab	12.10a	11.60A	10.80b	11.00ab	11.40ab	11.70a	11.20A
		Mean	10.00C	10.20C	10.60B	10.90A		8.90C	9.70B	10.10AB	10.50A	
Pod number per plant	Fe	Control	16.20 i	16.70 i	17.80 h	18.20 g	17.20C	15.1 h	16.2 g	16.4 g	17.2 f	16.20C
		3	18.70g	19.00f	20.20e	23.40d	20.30B	17.90f	18.30e	19.40d	19.90d	18.80B
		6	23.90d	24.60c	25.60b	26.30ab	25.10A	20.10c	20.10c	21.20b	23.00a	21.10A
		9	24.40c	25.10b	26.10ab	26.80a	25.60A	20.60c	20.60c	21.70b	23.70a	21.70A
		Mean	20.80D	21.30C	22.40B	23.60A		18.40C	18.80C	19.60B	21.00A	
Pod diameter (cm)	Fe	Control	0.51f	0.56e	0.57d	0.59d	0.55D	0.52 f	0.57 e	0.59 de	0.60 d	0.57D
		3	0.61c	0.62c	0.64c	0.69c	0.64C	0.61d	0.62d	0.67c	0.69c	0.64C
		6	0.70b	0.71b	0.73b	0.76b	0.72B	0.70c	0.73b	0.74b	0.79ab	0.74B
		9	0.81ab	0.83ab	0.85ab	0.91a	0.85A	0.81ab	0.83ab	0.85ab	0.87a	0.84A
		Mean	0.65C	0.68B	0.69B	0.73A		0.66B	0.68B	0.71A	0.73A	
Pod fresh weight (g)	Fe	Control	4.10f	4.50e	4.70e	5.10d	4.60D	3.90 e	4.10 e	4.30 de	4.40 d	4.10C
		3	5.20d	5.30d	5.60c	5.90b	5.50C	4.50cd	4.60c	4.80bc	5.10b	4.70C
		6	6.00b	6.10b	6.50ab	6.80ab	6.30B	5.20b	5.40b	5.60ab	5.90ab	5.50B
		9	6.50ab	6.60ab	7.00a	7.30a	6.90A	5.60ab	5.80ab	6.00a	6.30a	6.00A
		Mean	5.40C	5.60C	5.90B	6.20A		4.80C	4.90C	5.10B	5.40A	
Pod dry weight (g)	Fe	Control	1.10 h	1.40g	1.70f	1.90e	1.52D	0.90f	1.10f	1.30e	1.40e	1.10D
		3	2.00e	2.10e	2.50d	2.70cd	2.30C	1.50e	1.60de	1.90d	2.10c	1.70C
		6	2.80c	2.90c	3.10c	3.40b	3.00B	2.20c	2.30c	2.60bc	2.80b	2.40B
		9	3.50b	3.70ab	3.90a	4.10a	3.80A	2.90b	3.10b	3.30ab	3.60a	3.20A
		Mean	2.30D	2.50C	2.80B	3.00A		1.80D	2.00C	2.20B	2.40A	
Total yield per feddan (ton)	Fe	Control	3.10f	3.40f	3.60e	3.70e	3.40C	3.1 f	3.3 e	3.6 d	3.8 c	3.40D
		3	3.90d	4.10d	4.50c	4.70c	4.30B	3.90c	4.00bc	4.30bc	4.50b	4.10C
		6	4.90b	5.10b	5.30ab	5.60ab	5.20AB	4.60b	4.70b	5.10ab	5.40ab	4.90B
		9	5.20ab	5.40ab	5.60ab	5.90a	5.60A	5.00ab	5.20ab	5.60ab	5.90a	5.40A
		Mean	4.20C	4.50BC	4.70AB	4.90A		4.10C	4.30BC	4.60AB	4.90A	

.Means followed by different letters are significantly deferent at $P \leq 0.05$ level: Duncan's multiple range test.

Table (4): Effect of nano potassium and iron oxide foliar application on protein and fiber percentage as well as total soluble solids percentage of green bean pods during 2019 and 2020 seasons.

Characters	Season		First season					Second season				
	Treatments	(ml/l)	K					K				
			Control	2	4	8	Mean	Control	2	4	8	Mean
Protein (%)		Control	14.90i	15.30h	15.80h	16.30b	15.50D	15.40i	15.60i	15.90i	16.40h	15.80D
		3	17.60g	18.90fg	19.90fg	20.10f	19.10C	17.90g	18.60f	19.60e	21.20e	19.30C
	Fe	6	23.20e	25.60de	26.10d	26.90d	25.40B	23.50de	25.60d	26.30c	27.60b	25.70B
		9	27.20c	27.60c	28.10b	29.60a	28.10A	28.10ab	28.60ab	29.10a	26.50c	28.00A
		Mean	20.70D	21.80C	22.40B	23.20A		21.20C	22.10B	22.70AB	22.90A	
Fibers (%)		Control	7.50a	7.10ab	6.60b	6.30b	6.80A	8.10a	7.90ab	6.40b	6.10b	7.10A
		3	5.40cd	5.10d	4.90d	4.50e	4.90B	5.40bc	5.20c	5.10c	4.20d	4.90B
	Fe	6	4.60ef	4.10f	4.00f	3.90f	4.10B	3.70de	3.60de	3.50e	3.30f	3.50C
		9	3.60g	3.50h	3.40h	3.10i	3.40C	3.10g	2.90g	2.80h	2.40i	2.80D
		Mean	5.20A	4.90B	4.70C	4.40D		5.00A	4.90B	4.40C	4.00C	
Total soluble solids (%)		Control	2.30i	2.70h	3.10g	3.40f	2.80D	2.40i	2.90h	3.10g	3.30g	2.90D
		3	3.50f	3.80e	3.90de	4.00d	3.80C	3.60f	3.70f	3.90e	4.20d	3.80c
	Fe	6	4.10d	4.50c	4.70c	4.90bc	4.50B	4.40c	4.60c	4.80bc	4.90bc	4.60B
		9	5.10b	5.30b	5.70ab	5.90a	5.50A	5.10b	5.40b	5.70ab	6.10a	5.50A
		Mean	3.70C	4.00B	4.30AB	4.50A		3.80D	4.10C	4.30B	4.60A	

.Means followed by different letters are significantly deferent at $P \leq 0.05$ level: Duncan's multiple range test.

Table (5): Effect of nano potassium and iron oxide foliar application on potassium (%) and iron concentration (ppm) in green bean pods during 2019 and 2020 seasons.

Characters	Season		First season					Second season				
	Treatments	(ml/l)	K					K				
			Control	2	4	8	Mean	Control	2	4	8	Mean
Potassium (%)		Control	1.51i	1.54i	1.57h	1.61h	1.55D	1.56i	1.62h	1.67gh	1.69g	1.63D
		3	1.78f	1.85f	1.95ef	1.99e	1.89C	1.72f	1.75f	1.83ef	1.85e	1.78C
	Fe	6	2.11d	2.45cd	2.64c	2.78bc	2.49B	1.89d	1.94cd	1.97c	2.10bc	1.97B
		9	2.82b	2.91ab	2.94ab	3.10a	2.94A	2.19b	2.28ab	2.76ab	2.85a	2.52A
		Mean	2.05D	2.18C	2.27B	2.37A		1.84D	1.89C	2.05B	2.12A	
Iron (ppm)		Control	61.12i	62.31i	64.56hi	67.23h	63.80D	63.20i	64.11h	65.34g	67.45f	65.00D
		3	69.21g	70.12g	71.33f	72.122	70.69C	69.21f	70.13e	70.98e	71.23de	70.38C
	Fe	6	73.34d	75.67cd	76.45c	77.34bc	75.70B	72.34d	73.45cd	75.34c	76.45d	74.39B
		9	78.12b	79.34ab	79.84ab	81.23a	79.63A	77.45b	78.34ab	78.78ab	79.11a	78.42A
		Mean	70.44D	71.86C	73.04B	74.48A		70.55D	71.50C	72.61B	73.56A	

.Means followed by different letters are significantly deferent at $P \leq 0.05$ level: Duncan's multiple range test.

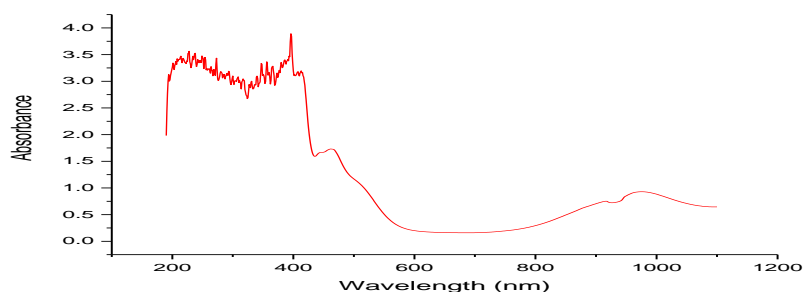


Figure 8: UV spectra of PVP/ iron oxide

The formation of iron oxide was monitored/confirmed by UV-Vis spectroscopy as shown in Figure 8. UV analysis of iron oxide nanoparticles embedded in PVP/ acetic acid/ glycerine solution displays three characteristic absorption bands at 224, 395 and 460 nm; due to surface plasmon, which signifies the conversion of ferrous sulfate solution as an iron precursor to iron oxide nanoparticles. This broad absorption is the consequence of different electronic transitions: Fe(III) crystal transitions, magnetically coupled Fe(III) interactions and oxygen-iron charge transfer excitations from O(2p) nonbonding valence bands to the Fe(3d) ligand field orbitals. The charge transfer transitions involving Fe^{III}-O are mainly responsible for absorption of visible light. It also signifies that the gamma radiation-induced polymerization of PVP is a successful method for reducing the ferrous ions to iron oxide nanoparticles. The results are in agreement with studies carried out by other researchers reported in literature [52]. Finally, the peak presented at 978 nm is assigned for O-H from water.

Agricultural study

Vegetative growth characters.

Data presented in Table (2) show that both concentrations 4 and 8 ml/l of nano potassium gave the highest number of leaves, number of branches and plant dry matter percentage, while plants sprayed with 8ml/l of nano potassium alone gave higher plant length, total plant fresh weight and chlorophyll reading than other concentrations in both seasons.

On the other hand, it was found that spraying green bean plants with 9ml/l of nano iron oxide scored the highest plant length, number of leaves and branches, total plant fresh weight, dry matter and chlorophyll reading in both seasons. Similar results were obtained by El-Zawily *et al.* [53] who found that the application of highest nano potassium concentration increase plant height, leaf number per plant and dry matter as well as scored the highest chlorophyll reading of cucumber plants. As for nano iron oxide, similar results were obtained by Abdel-Salam[54] who found that spraying faba bean plants with nano iron oxide led to an increase in plant height, Rui *et al.* [55]who declared that the foliar application with nano iron oxide increased chlorophyll content of pea nut plants.

Respecting the interaction between both nano elements, data revealed that the combination among 4 and 8 ml/l of nano potassium as well as 9 ml/l of nano iron oxide scored the highest values of plant length and number of leaves in both seasons and the same previous concentrations of nano potassium plus 2 ml/l of the same element combined with 9 ml/l of nano iron oxide gave the highest number of branches during the two successive seasons. As for total plant fresh weight and dry matter percentage, data show that 8 ml/l of nano potassium and 6ml/l as well as 9 ml/l of nano iron oxide gave the highest values for both characters. Respecting chlorophyll reading, it was observed that 8 ml/l of nano potassium and 9 ml/l of nano iron oxide gave higher chlorophyll reading than other treatments in both seasons. The simulative effect of nano potassium on vegetative characters might be attributed to its role on enhancing

and stimulating the activity of different enzymes which play an important role in metabolic process such as carbon process and cell division [56]. Also, it might be attributed to the high activity of nano potassium which has better physical and chemical properties, high surface area than traditional potassium, which referred to its highly surface area that gave plants better chance to absorb the element and enhance the metabolic process, increasing enzymes activity of photosynthesis and chlorophyll content [57] which reflect on growth characters such as plant length, leaves and branches number, plant fresh and dry weight. Also nano potassium play an important role in the facilitation of cell-to cell translocation through the plasmodesmata [58].

Concerning the simulative effect of nano iron oxide on plant growth, it might be referred to its important role in some physiological process such as respiration, production and formation of plant hormones, vital process and biosynthesis of chlorophyll [59] which reflect on plant growth characters.

Green pod yield and its components.

As for green pod yield and its components, data tabulated in Table (3) show that green bean plants sprayed with 8 ml/l of nano potassium gave the highest pod length, number of pods per plant, pod fresh and dry weight, while untreated plants scored the lowest pod diameter during the two successive seasons.

On the other hand, it was marked that both concentrations 4 and 8ml/l of nano potassium led to the highest total yield per feddan in both seasons. These results agree with that obtained by El-Zawily *et.al.*[53] and Panda *et al.* [60] who observed that the highest concentration of nano potassium increase total fruit weight and total fruit number of cucumber plants and fruit weight and total yield of tomato.

As for the effect of nano iron oxide, data show that green bean plants sprayed with 9 ml/l of nano iron oxide scored the highest pod length, pod diameter, pod fresh and dry weight as well as total yield per feddan in both seasons. As for pod number per plant, the foliar application with 6 ml/l and 9ml/l of nano iron oxide scored the highest value in the first and the second seasons. Similar result was obtained by Sheykhbaglou *et al.* [61] and Abdel-Salam [54] who found that nano iron oxide had a positive effect on increasing pod dry weight of soybean plants and pod number per plant of faba bean.

Concerning the interaction between both elements' foliar application, data revealed that the foliar application with 2ml/l, 4ml/l and 8 ml/l of nano potassium combined with 9ml/l of nano iron oxide scored the highest pod length in both seasons.

As for pod number per plant, it was found that spraying green bean plants with 8 ml/l of nano potassium combined with 6ml/l and 9 ml/l of nano iron oxide gave the highest pod number per plant during the two successive seasons. Regarding pod diameter, data revealed that all concentrations of nano potassium combined with 3 ml/l of nano iron oxide led to the lowest pod diameter in both seasons.

As for pod fresh and dry weight, it could be concluded that plants sprayed with 4ml/l and 8ml/l of nano potassium combined with 6 ml/l of nano iron oxide and all concentrations of nano potassium combined with 9 ml/l of nano iron oxide yielded the highest pod fresh and total yield per feddan, while the interaction among 4ml/l and 8 ml/l of nano potassium combined with 9 ml/l of nano iron oxide scored the highest pod dry weight in both seasons. This result might be referred to the effect of nano potassium that increase enzymes activity of photosynthesis and chlorophyll content [62] which enhance the photosynthesis process, also its important role in the translocation of the output of the photosynthesis process and carbohydrates from leaves to different storage organs and fruits which reflect on pod yield and its components [63]. From another point the simulative effect of nano potassium might be referred to its role on enhancing the physiological process in plant such as enzymatic and vital reactions and regulating hormones production [64]. As for nano iron oxide, its positive effect on pod yield might be attributed to its role in synthesis of plant hormones, vital process and biosynthesis of chlorophyll [59], which reflect on plant growth characters as presented in Table (3) which lead to an increase on total yield.

Nutritional value.

As for nutritional value in green pods, data presented in Table (4) show that spraying green bean plants with 8 ml/l of nano potassium and 9 ml/l of nano iron oxide scored the highest percentage of protein and total soluble solids in both seasons. As for fiber percentage in green pods, data illustrated that plants sprayed with 4 ml/l of nano potassium and 9 ml/l of nano iron oxide led to the lowest percentage during the two successive seasons. Concerning the interaction between both elements, it was observed that the combination between 8 ml/l and 4 ml/l of nano potassium and 9 ml/l of nano iron oxide scored the highest protein percentage in the first and the second season respectively.

On the other side, data show that 8 ml/l of nano potassium combined with 9 ml/l of nano iron oxide yielded the lowest fiber percentage in green pods in both seasons. Regarding total soluble solids percentage, the interaction among 4 ml/l and 8 ml/l of nano potassium as well as 9 ml/l of nano iron

oxide gave the highest percentage in both seasons. This result agrees with that obtained by Delfani *et al.* [13] who found that black eyed pea sprayed with nano iron oxide scored the highest protein percentage in seeds.

The effect of nano fertilizers on enhancing the nutritional value of green pods might be referred to its physical characters and properties, whereas nano fertilizers have a good penetration cause they have low particles size (below 100 nm) which are lower than stomata size of leaves and gave the opportunity to penetrate and gave more chance of use efficiency than traditional fertilizer and increase the metabolic process which reflect on chemical constituents [65]. Also, potassium has an important catalytic role in protein synthesis and all enzymes which play a critical role on regulating all growth process [66]. From another point potassium has a considerable role in the translocation of carbohydrates from leaves to storage organs (fruits) which led to an accumulation of sugars and increase the T.S.S. percentage [67]. As for the effect of simulative effect of nano iron oxide on chemical constituents of green pods, it might be referred to the necessary role of iron on enhancing the formation and the symbiotic relation which reflect on enhancing the fixation of nitrogen [68]. Nitrogenase enzyme is the main factor which play an important role in the conversion of atmospheric nitrogen to ammonia through two essential components which are composed from iron protein which is reduced then outfit molybdenum-iron protein with electrons that contain the catalytic site [69].

As for potassium percentage and iron concentration in green beanpods, data tabulated in Table (5) show that plants sprayed with 8ml/l of nano potassium and 9 ml/l of nano iron oxide scored the highest percentage and concentration of both elements in green pods during the two successive seasons. On the other hand, data illustrated that the combination between 8 ml/l of nano potassium and 9 ml/l of nano iron oxide led to the highest percentage of potassium and iron concentration in green pods in the first and the second seasons. Similar finding was obtained by Abd El-Azeim *et al.* [70] who found that the highest concentration of nano potassium foliar application scored the highest percentage of potassium content in potato tubers. Also, Ruet *al.* [55] who found that peanut plants treated with high concentration of nano iron oxide scored the highest concentration of iron in roots and shoots. Previous study show that nano elements have the opportunity to translocate and penetrate to different plant organs as a result of their nano size which is lower than plant stomata and pore size of cells which lead to the

accumulation of different nano elements in plant organs.

Conclusion.

It could be concluded that the successful formation of potassium and iron oxide nanoparticles inside the PVA and PVP networks, respectively via gamma irradiation according to the data obtained from HRTEM, UV-vis spectroscopy, and FTIR, PVA and PVP act as good stabilizers which control the growth and crystalline phase formation of potassium and iron oxide nanoparticles. From another side, the foliar application with 8 ml/l and 9ml/l of nano potassium and nano iron oxide respectively have a positive effect on growth characters which reflect on pod yield and its chemical constituents.

Conflicts of interest.

There are no conflicts to declare

Acknowledgments.

The authors are grateful for the support of both National Centre for Radiation Research and Technology and National Research Center for facilitating the laboratory and agricultural experiments.

References

- [1] H.El-Ramady, A. El-Ghamry, A. Mosa, T. Alshaa, Nanofertilizers vs. biofertilizers: new insights, Environment, Biodiversity and Soil Security, 2 (2018) 40-50, DOI:10.21608/JENVBS.2018.3880.1029.
- [2] J.C. Tarafdar, R. Raliya, H. Mahawar, I. Rathore, Development of zinc nanofertilizer to enhance crop production in pearl millet (*Pennisetum americanum*), Agriculture Research Journal, 3(3) (2014) 257-262, DOI:10.1007/s40003-014-0113-y.
- [3] P.K. Mani, S. Mondal, Agri-nanotechniques for plant availability of nutrients, Plant Biotechnology Journal, (2016) 263-303, DOI:10.1009/978-3-319-42154-4 11.
- [4] P.L.Kashyap, X. Xiang, P. Heiden, Chitosan nanoparticle based delivery systems for sustainable agriculture, International Journal of Biological Macromolecules, (77) (2015) 3651, DOI:10.1016/j.ijbiomac.2015.02.039.
- [5] M.R. Castiglione, R. Cremonini, Nanoparticles and higher plants, Caryologia, 6 (2009) 161-165, DOI:10.1080/00087114.2004.10589681.
- [6] M. Ghorbanpour, K. Manika, A. Varma, Nano-science and plant-soil systems, Springer International publishing, (2017) 1-552.
- [7] M.M. Merghany, M.M. Shahein, S. Mahmoud, K.F. Abdelgawad, A.F. Radwan, Effect of nano-fertilizers on cucumber plant growth, fruit yield and its quality, Plant Archives, 19 (2) (2019) 165-172.

- [8] R. Lal, Promise and limitations of soils to minimize climate change, *Journal of Water and Soil Science*, 63 (4) (2008) 113A-118A, DOI:10.2489/jswc.63.4.113A.
- [9] I. Khan, K. Saeed, I. Khan, Nanoparticles: properties, applications and toxicities, *Arabian Journal of Chemistry*, 12 (7) (2019) 908-931.
- [10] I. M.R. Nader, A. Abedi, Application of nanotechnology in agriculture and refinement of environmental pollutants, *Journal of Nanotechnology*, 11(1) (2012)18-26.
- [11] M.V. Khodakovskaya, K. De Silva, A.S. Biris, E. Dervishi, H. Villagarcia, Carbon nanotubes induce growth enhancement of tobacco cells, *ACS Nano*, 6(3) (2012) 2128-2135, DOI:10.1021/nn204643g.
- [12] A. Fleischer, A. Malcolm, O'Neill, R. Ehwald, The pore size of non-graminaceous plant cell walls is rapidly decreased by borate ester cross-linking of the pectic polysaccharide Rhamnogalacturonan, *Plant Physiology*, 121(3) (1999) 829-838, DOI:10.1104/pp.121.3.829.
- [13] M. Delfani, M.B. Firouzabadi, N. Farrokhi, H. Makarian, Some physiological responses of black-eyed pea to iron and magnesium nano fertilizers, *Communications in Soil Science and Plant Analysis*, 45(2014) 530-540, DOI:10.1080/00103624.2013.863911.
- [14] J.F. Briat, C. Dubos, F. Gaymard, Iron nutrition, biomass production, and plant product quality, *Trends in Plant Science*, 20 (33) (2015)33-40, DOI:10.1016/j.tplants.2014.07.005.
- [15] H.J. Suh, C.S. Kim, J.Y. Lee, J. Jung, Photodynamic effect of iron excess on photosystem II function in pea plants, *Photochemistry*, 75(2002) 513-518, DOI:10.1562/0031.
- [16] B.S. Sekhon, Nanotechnology in agri-food production: an overview, *Nanotechnology, Science and Applications*, 7(2014)31-53, DOI:10.2147/NSA.S39406.
- [17] P.S. Bindraban, C. Dimkpa, L. Nagarajan, A. Roy, R. Rabbinge, Revisiting fertilizers and fertilization strategies for improved nutrient uptake by plants, *Biology and Fertility of Soils*, 51(2015)897-911, DOI:10.107/s00374-01501039-7.
- [18] L. Ye, L. Li, L. Wang, S. Wang, S. Li, J. Du, S. Zhang, H. Shou, MPK3/MPK 6 are involved in iron deficiency- induced ethylene production in Arabidopsis, *Frontiers of plant Science*, 6 (953) (2015)1-10, DOI:10.3389/fpls.2015.00953.
- [19] F. Sultana, M. Manirujjaman, U. Imran, M.A. Haque, S. Sharmin, An overview of nanogel drug delivery system, *Journal of Applied Pharmaceutical Science*, 3 (2013) 95-105, DOI:10.7324/JAPS.2013.38. S15.
- [20] S. Kadlubowski, Radiation-induced synthesis of nanogels based on poly (N-vinyl-2-pyrrolidone)-a review, *Radiation Physics and Chemistry*, 102(2014) 29-39, DOI:10.1016/j.radphyschem.2014.04.016.
- [21] J. Pandey, A. Shukla, Synthesis and characterization of PVDF supported silica immobilized phosphotungstic acid (Si-PWA/ PVDF) ion exchange membrane, *Materials letters*, 100 (2013)292-295, DOI:10.1016/j.matlet.2013.03.039.
- [22] S. Ahlberg, A. Antonopolus, J. Diendorf, R. Dringen, M. Eppe, R. Flöck, PVP-coated, negatively charged silver nanoparticles: a multi-center study of their physicochemical characteristics, cell culture and in vivo experiments, *Beilstein journal of nanotechnology*, (5) (2014) 1944-1965, DOI:10.3762/bjnano.5.205.
- [23] S.O. Aisida, I. Ahmad, T.K. Zhao, M. Maaza, F.I. Ezema, Calcination effect on the photoluminescence, optical, structural, and magnetic properties of polyvinyl alcohol doped Zn Fe₂O₄ nanoparticles, *Journal of Macromolecular Science Part B*, 59(2020)295-308, DOI:10.1080/00222348.2020.1713519.
- [24] A. Kyrchenko, D.A. Pasko, O.N. Kalugin, Poly (vinyl alcohol) as a water protecting agent for silver nanoparticles: the role of polymer size and structure, *Physical Chemistry Chemical Physics*, 19 (2017). 8742-8756, DOI: 10.1039/C6CP05562A.
- [25] FAOSTAT, Green Bean World Statistics. Major food and agricultural commodities producers-Countries by commodity. Available online: www.faostat.fao.org (accessed on 23 October) (2017).
- [26] A.A. El-Noemani, H.A. El-Zeiny, A.M. El-Gindy, E.A. El-Sahhar, M.A. El-Shawadfy, Performance of some bean (*Phaseolus vulgaris* L.) varieties under different irrigation systems and regimes, *Australian Journal of Basic and Applied Sciences*, 4 (2010) 6185-6196.
- [27] N.A. Hamed, M. Salah, F. Ahmed, T. Shoala, Physiological assessment of radiation and PVP/ Zn nanoparticles on sour orange seedling, *Asian Journal of Agricultural and Horticultural Research*, 4(4) (2019)1-18, DOI:10.9734/ajahr/2019/v4i430033.
- [28] K.G. Helmy, A.M. Partila, M. Salah, Gamma radiation and polyvinyl pyrrolidone mediated synthesis of zinc oxide / zinc sulfide nanoparticles and evaluation of their antifungal effect on pre and post harvested orange and pomegranate fruits, *Bio catalysis and Agricultural Biotechnology*, 29 (2020) 1-12, DOI:10.1016/j.bcab.2020.101728.
- [29] A.O.A.C. Official Methods of Analysis. 15th ed. Association of Official Analytical Chemists, Arlington, VA (1990).
- [30] S.N. Rai, V.D. Mudgal, Synergistic effect of sodium hydroxid and steam pressure treatment on compositional changes and fiber utilization of wheat straw, *Biological wastes*, 24(1988)105-114.
- [31] J. Brown, O. Lillel, Rapid determination of potassium and sodium in plant material and soil extracts by flame photometric, *Proceedings of the American Society for Horticultural Science*, 48(1946) 341-346.
- [32] H.D. Chapman, P. E. Pratt, *Methods of analysis for soil, plant and waters*. University of California. Department of Agricultural Science, USA, (1978) 1-309.
- [33] MSTAT Development Team. MSTAT user's guide: A microcomputer program for the design, management and analysis of agronomic research experiments. Michigan State University East Lansing, U.S.A (1989).
- [34] R.G.D. Steel, J.H. Torrie, *Principles and Procedures of Statistics*, McGraw Hill, New York. (1980).
- [35] A.A. Álvaro, D. Queiroz, E.D. Passos, S.D.B. Alves, G.S. Silva, O.Z. Higa, M. Vi'tolo, Alginate-poly (vinyl alcohol) core-shell microspheres for lipase immobilization, *Journal of Applied Polymer Science*, 102 (2006) 1553-1560, DOI:10.1002/app.23444.

- [36] P. Sheoran, S. Goel, R. Boora, S. Kumari, S. Yashveer, S. Grewal, Biogenic synthesis of potassium nanoparticles and their evaluation as a growth promoter in wheat, *Plant Gene*, 27 (2021)1-8, DOI:10.1016/j.plgene.2021.100310.
- [37] E.C. Olivares, J.L. Olivares-Romero, F. Barrera-Méndez, Micro encapsulation of potassium phosphate in chitosan and the effect of spray drying operating variables on the particle size, *Journal of the Mexican Chemical Society*, 62(3) (2018) 67-74, DOI:10.29356/jmcs.v62i3.452.
- [38] T. Ahmed, S. Balendhran, N. Karim, E.L.H. Mayes, Degradation of black phosphorus is contingent on UV-blue light exposure, *npj 2D Materials and Applications*, (2017)1-7. DOI: 10.1038/s41699-017-0023-5.
- [39] C. Amgoth, A. Singh, R. Santhosh, S. Yumnam, P. Mangla, R. Karthik, T. Guping, M. Banavoth, Solvent assisted size effect on Au NPs and significant inhibition on K562 cells, *RSC Advances*, 9(2019) 33931-33940, DOI:10.1039/c9ra05484g.
- [40] A.A.H. Hernández, G.A. Álvarez, R.C. Cortés, M. H. Luis, M. Huizar, R.J. Alvarado, Iron oxide nanoparticles: synthesis, functionalization, and applications in diagnosis and treatment of cancer, *Chemical Papers*, 74(2020)3809-3824, DOI: 10.1007/s11696-020-01229-8.
- [41] I. Karimzadeh, M. Aghazadeh, M.R. Ganjali, T. Doroudi, P.H. Kolivand, Preparation and characterization of iron oxide (Fe₃O₄) nanoparticles coated with polyvinylpyrrolidone/polyethylenimine through a facile one-pot deposition route, *Journal of Magnetism and Magnetic Materials*, 433 (2017)148-154, DOI:10.1016/j.jmmm.2017.02.048.
- [42] S.H. Chaki, T.J. Malek, M.D. Chaudhary, J.P. Tailor, M.P. Deshpande, Magnetite Fe₃O₄ nanoparticles synthesis by wet chemical reduction and their characterization, *Advances in Natural Sciences, Nano science and Nanotechnology*, 6 (2015) 1-6, DOI: 10.1088/2043-6262/6/3/035009.
- [43] K. Seo, K. Sinha, E. Novitskaya, O.A. Graeve, Polyvinylpyrrolidone (PVP) effects on iron oxide nanoparticle formation, *Materials letters*, 215(2018)203-206, DOI:10.1016/j.matlet.2017.12.107.
- [44] M. Eid, M.B. El-Arnaouty, M. Salah, E. Soliman, E.S.A. Hegazy, Radiation synthesis and characterization of poly (vinylalcohol)/poly (N-vinyl-2-pyrrolidone) based hydrogels containing silver nanoparticles, *Journal of Polymer Research*, 19(2012) 1-10, DOI:10.1007/s10965-012-9835-3.
- [45] M.B. El-Arnaouty, M. Eid, M. Salah, E.S.A. Hegazy, Preparation and characterization of poly vinyl alcohol/poly vinyl pyrrolidone/clay based nano composite by gamma irradiation, *Journal of Macromolecular Science*, (49) (2012) 1041-1051, DOI:10.1080/10601325.2012.728466.
- [46] M. Eid, M.B. El-Arnaouty, M. Salah, E. Soliman, E.S.A. Hegazy, Radiation synthesis and characterization of poly (aniline/glycidyl methacrylate) - Ag₂O nano composites, *Inorganic chemistry communications*, 114 (2020) 1-10. DOI: 10.1016/j.inoche.2020.107844.
- [47] R. M. L. Helberg, Z. Dai, L. Ansaloni, L. Deng, PVA/PVP blend polymer matrix for hosting carriers in facilitated transport membranes: Synergistic enhancement of CO₂ separation performance, *Green Energy and Environment*, 5(2020)59-68, DOI: 10.1016/j.gee.2019.10.001.
- [48] M.B. El-Arnaouty, M. Eid, M. Salah, E. Soliman, E.A. Hegazy, Synthesis of poly (aniline/glycidyl methacrylate)-TiO₂ nano composites via gamma irradiation and their electro-responsive characteristic, *Journal of Inorganic and Organometallic Polymers and Materials*, 27 (2017) 1482-1490, DOI:10.1007/s10904-017-0607-8.
- [49] S. Saif, A. Tahir, T. Asim, Y. Chen, S.F. Adil, Polymeric nanocomposites of iron-oxide nanoparticles (IONPs) synthesized using Terminalia chebula leaf extract for enhanced adsorption of arsenic (V) from water, *Colloids Interfaces* 3(17) (2019) 1-20, DOI:10.3390/colloids3010017.
- [50] M. Salah, M. Gad, M. Elkattan, Y.M. Sabry, Optical constants of gamma-irradiated silver-doped PVA in the near-infrared range, *Micro and Nano Letters*, 15 (7) (2020a) 480-485, DOI:10.1049/mnl.2019.0800.
- [51] M. Salah, M. Gad, M. Elkattan, Y.M. Sabry, Effect of gamma-irradiation and doping on the absorption edge and the optical band gap of silver-doped PVA films, *Optics communications*, 473(2020b) 1-7, DOI:10.1016/j.optcom.2020.125933.
- [52] I. Rosli, H. Zulhaimi, S. Ibrahim, S. Gopinath, K. Kasim, H. M. Akmal, A. Nuradibah, T. S. Sam, phytosynthesis of iron nanoparticle from averrhoabilimbinin, *Materials Science and Engineering*, 318 (2017)1-10, DOI:10.1088/1757-899X/318/1/012012.
- [53] A.I. El-Zawily, M.B.I. El-Sawy, E.M.H. EL-Semellawy, R.S.A. Abd-El-Ghaffar, Effect of magnetization and nano potassium particles on growth, yield and fruit quality of cucumber under plastic house conditions, *Journal of Productivity and Development*, 23(3) (2018)627- 652, DOI: 10.21608/jpd.2018.42548.
- [54] M.A. Abdel-Salam, Implications of applying nano-hydroxyapatite and nano-iron oxide on Faba bean (*Vicia faba* L.) productivity, *Journal of Soil Sciences and Agricultural Engineering*, 9 (11) (2018)543-548, DOI:10.21608/jssae.2018.36469.
- [55] M.Z. Rui, C. Ma, Y. Hao, J. Guo, Y. Rui, X. Tang, Q. Zhao, X. Fan, Z. Zhang, T. Hou, S. Zhu, Iron oxide nanoparticles as a potential iron fertilizer for peanut (*Arachis hypogaea*), *Frontiers of Plant Science*, 7 (815) (2016) 1-10, DOI:10.3389/fpls.2016.00815. *Frontiers of plant science*.
- [56] J.L. Havlin, J.D. Beaton, S.L. Tisdale, W.L. Nelson, Soil fertility and fertilizers, in an introduction to nutrient management. 6th ed. Prentice Hall, New Jersey, (2005)199-218.
- [57] E. Morteza, P. Moaveni, H.A. Farahani, M. Kiyani, Study of photosynthetic pigments changes of maize (*Zea mays* L.) under nano TiO₂ spraying at various growth stages, Springer Plus, (2013)247-249, DOI: 10.1186/2193-1801-2-247.
- [58] P. Zambryski, Cell-to-cell transport of proteins and fluorescent tracers via plasmodesmata during plant development, *Journal of Cell Biology*, 162 (2) (2004)165-168, DOI:10.1083/jcb.200310048.

- [59] M. Mohammadi, N.M. Hoseini, M.R. Chaichi, H. Alipour, M. Dashtak, S. Safikhani, Influence of nano-iron oxide and zinc sulfate on physiological characteristics of peppermint, *Communications in Soil Science and Plant Analysis*, 49(18) (2018) 2315-2326, DOI:10.1080/00103624.2018.1499766.
- [60] J. Panda, A. Nandi, S.P. Mishra, A.K. Pal, A.K. Pattnaik, N.K. Jena, Effects of nano fertilizer on yield, yield attributes and economics in tomato (*Solanum Lycopersicum L.*), *International Journal of Current Microbiology and Applied Sciences*, 9(5) (2020) 25832591, DOI:10.20546/ijcmas.2020.905.295.
- [61] R. Sheykhbaglou, M. Sedghi, M.T. Shishevan, R.S. Sharifi, Effects of nano-iron oxide particles on agronomic traits of soybean, *Notulae Scientiae Biologicae*, 2 (2) (2010) 112-113, DOI:10.15835/nsb.2.2.4667.
- [62] Z.A. Siddiqui, M.S. Akhtar, K. Futai, *Mycorrhizae: Sustainable agriculture and Forestry*. Springer, Netherlands, (2008) 287-302, DOI:10.1007/978-1-4020-8770-7.
- [63] J.W. Patrick, W.S.D. Zhang, C.E. Offer, N.A. Walker, Role of membrane transport in phloem translocation of assimilates and water, *Australian Journal of Plant Physiology*, 28 (2001) 695-707, DOI:10.1071/PP01023.
- [64] M. Grover, S. Singh, B. Teswarlu, Nanotechnology: scope and limitations in agriculture, *International Journal of Nanotechnology and Applications*, 2(1) (2012) 10-38.
- [65] D. Lairon, Nutritional quality and safety of organic food a review, *Agronomy for Sustainable Development*, 30 (1) (2009) 33-41, DOI: 10.1051/agro/2009019.
- [66] R.B. Patil, Role of potassium humate on growth and yield of soybean and black gram, *International Journal of Pharma and Bio Sciences*, 2 (1) (2011) 242-246.
- [67] G.E. Lester, J.L. Lifon, D.J. Makus, Impact of potassium nutrition on postharvest fruit quality: Melon (*Cucumis melo L.*) case study, *Plant Soil*, 335(2010) 113-117, DOI: 10.1007/s11104-009-0227-3.
- [68] E.M. Brear, D.A. Day, P.M.C. Smith, Iron: an essential micronutrient for the legume-rhizobium symbiosis, *Frontiers of plant science*, 4(359) (2013) 1-16, DOI: 10.3389/fpls.2013.00359.
- [69] R. Dixon, D. Kahn, Genetic regulation of biological nitrogen fixation. *Nature reviews, Microbiology*, 2 (2004) 621-631 (2004), DOI: 10.1038/nrmicro954.
- [70] M.M. Abd El-Azeim, M.A. Sherif, M.S. Hussien, I.A.A. Tantawy, S.O. Bashandy, Impacts of nano- and non-nanofertilizers on potato quality and productivity, *Acta Ecologica Sinica*, 40 (5) (2020) 1-10, DOI:10.1016/j.chnaes.2019.12.007.